Observation of Temporal Solitons in Second-Harmonic Generation with Tilted Pulses

P. Di Trapani,[1,*] D. Caironi,[2] G. Valiulis,[3] A. Dubietis,[3] R. Danielius,[3] and A. Piskarskas[3]
[1]*Institute of Mathematical, Physical and Chemical Sciences, University of Milano, via Lucini 3, 22100 Como, Italy and INFM (Istituto Nazionale per la Fisica della Materia), Milano, Italy*
[2]*Faculty of Sciences, University of Milano, 20100 Milano, Italy*
[3]*Department of Quantum Electronics, Vilnius University, 2040 Vilnius, Lithuania*
(Received 14 November 1997)

By eliminating the group-velocity mismatch and enhancing the group-velocity dispersion *via* pulse-front tilting, we obtained the formation of temporal solitary waves in phase-mismatched second-harmonic generation. Experimental and numerical results match well in a wide range of intensities and Δk's. In a 7 mm BBO crystal, 58 fs, 527 nm pulses are obtained starting from 200 fs pump, at the same wavelength. [S0031-9007(98)06628-9]

PACS numbers: 42.65.Tg, 03.40.Kf, 42.65.Ky, 42.65.Re

Traveling-wave parametric interaction in $\chi^{(2)}$ nonlinear materials is becoming a subject of intense study owing to its potential applications in ultra-high speed all-optical processing. In fact, while the speed of resonator-based schemes is limited to the sub-ns regime by the feedback buildup time, that of traveling-wave devices is defined only by the shortest usable pulses. This may allow the development of optical amplifiers, frequency mixers, beam/pulse reshapers, optical gates, optical transistors, and other all-optical processors capable of being operated above the THz frequency.

The property of solitons of being invariant under propagation and robust with respect to external perturbations makes them the most suitable means for processing bits of information. In the 1970s, Karamzin and Sukhorukov [1] addressed the possibility of obtaining spatial (or temporal) solitary waves in $\chi^{(2)}$ materials: beams propagating with constant or oscillating diameter (pulses with constant or oscillating duration) were obtained in analytical and numerical solutions of the three-wave coupled equations, by virtue of the competition between diffraction (or group-velocity dispersion, GVD) and $\chi^{(2)}$-induced self phase modulation.

More than 20 years of research on lasers and nonlinear materials were needed to obtain experimental evidence of $\chi^{(2)}$ spatial solitons, in the case of second-harmonic generation (SHG) in two dimensions (i.e., in bulk crystals [2]) or in 1D (i.e., in planar wave guides [3]), as well as in the case of 2D parametric amplification of incoherent quantum noise [4]. Concerning $\chi^{(2)}$ temporal solitons, several theoretical and numerical investigations have been performed, in which different kinds of solitonlike solutions and regimes of interaction have been investigated (see, for example, Refs. [5]). However, no experimental results have been presented to date and traveling-wave temporal solitons are commonly considered as difficult to be obtained in any of the presently available nonlinear materials (see, for example, Menyuk *et al.* and Torner *et al.* in Refs. [5]). The reason is the dominant role of the group-velocity mismatch (GVM), which splits the interacting pulses at different wavelengths before the interplay between gain and GVD allows the trapping mechanism to set in. To avoid this problem, one should use pulses so short ($\simeq$1 fs) as to make the effect of GVD ($\propto \tau^{-2}$) dominate over that of GVM ($\propto \tau^{-1}$), and so intense (several TW/cm^2) as to prevent the quenching of the parametric interaction due to large dispersion. Even if these operating conditions were achievable in real experiments, the higher order nonlinearities and dispersion that would be involved would remove the regime of interaction far from that in which $\chi^{(2)}$ solitons are supposed to be obtainable. This is not the case in the space domain, where the analog of GVM (i.e., the lateral walkoff) can be made small or even absent by operating close to [2], or exactly at [4], noncritical phase matching.

(A different class of χ^2 temporal solitons, which fulfill the elastic-scattering requirement, was predicted to be obtainable due to the interplay between gain and GVM [6]. This process, however, occurs only in transient regime and does not lead to the pulse compression, the mutual trapping and the (quasi-) stationary regime of propagation which are the main properties of GVD solitons, relevant to light-by-light applications. Moreover, such solitons are obtainable only with fairly long pulses, in conditions where the GVD plays a negligible role. We also note that the GVD behaves as a source of instability for the giant-pulse [7] (sometimes called soliton) formation, so much so that they are not obtainable in traveling-wave configurations [8].)

In this Letter we show that temporal solitons are experimentally obtainable in type-I (oo-e) SHG by using tilted pulses (with the amplitude front tilted respect to the phase front, as depicted in Fig. 1 of Ref. [9]). This is a consequence of the impact of tilt on effective GVM and GVD, which can be tuned to the proper values for soliton formation, in real materials. In fact, for suitable tilt, the contribution of the lateral walkoff to the collinear group velocity (GV) of the extraordinary-polarized (i.e., the SH) wave allows exact compensation of GVM, the GV of the ordinary wave being not affected by the tilt [10]. This

 0031-9007/98/81(3)/570(4)$15.00

effect was originally proposed, in a different form, by Martinez [11] and by Szabo *et al.* [12], for achieving the so-called "achromatic phase matching" in SHG with ultra broad-bandwidth pulses. It has also been used by some of the present authors to obtain efficient fs parametric generation [10] and to achieve fs pulse compression in second-harmonic [13] and third-harmonic generation [14].

Regarding the impact of tilt on GVD, it is known that it introduces anomalous dispersion [9], and dispersion-free propagation of tilted pulses in linear dispersive material has been demonstrated [15]. This is not what we are interested in, because high dispersion is needed for the soliton generation. However, suitable crystals and wavelength regions can be found for which the optimum tilt (that which provides exact GVM compensation, in SHG) also gives rise to suitable effective GVD for soliton generation. In this context, "suitable" means that it should lead to a soliton-pulse duration markedly shorter than that of the injected pulse, in order to prove the effect, but not too short, in order to allow the transient to be completed within the length of the available crystal. Several regimes, with large or small phase-mismatch (Δk) and with large or small GVD are obtainable for different crystals, pump-pulse durations, and wavelengths. Some of them are listed and compared in Ref. [16].

The experiment is aimed at demonstrating solitary wave propagation in SHG, in the regime of large Δk and small energy conversion (η). This choice is dictated by the requirement of avoiding relevant two-photon absorption at 264 nm [17], which would prevent the soliton generation. Note that this is one of the main theoretically investigated regimes because in this limit, in which the SH adiabatically follows the fundamental, the parametric equations reduce to the nonlinear Schrödinger equation, which admits exact soliton solution [5].

The nonlinear crystal used is a 7-mm long β-barium borate (BBO), operated in type I phase matching; the injected 200 fs, 527 nm pulses, in a 4 mm beam, are provided by a chirped-pulse amplified Nd:glass laser, followed by a nonlinear SH pulse compressor [18]. The input pulses were tilted by directing the laser beam onto a diffraction grating, whose face was imaged by a suitable telescope onto the entrance face of the BBO crystal (see the analogous setup depicted in Ref. [11]). The optics were set to achieve a tilt angle of 50°, inside the BBO; the values of the GVM and GVD coefficients corresponding to normal and tilted pulses are listed in Table I. The tilt of the output pulses was eliminated by a second telescope and grating, before sending the beam to the spectrometer and the scanning SH autocorrelator.

TABLE I. Impact of tilt on GVM ($\Delta k' = k'_\omega - k'_{2\omega}$) and GVD ($k''$) for SHG in BBO at 527 nm (fundamental).

Tilt [deg]	$k'_\omega - k'_{2\omega}$ [ps/mm]	k''_ω [ps^2/m]	$k''_{2\omega}$ [ps^2/m]
0	−0.589	0.138	0.4389
50	0	−1.825	−0.755

The process is modeled assuming that the evolution of the interacting tilted pulses is equal to that of plane pulses in a crystal with effective GVM and GVD coefficients as listed in Table I. The description is obtained by numerically solving the (degenerate) three-wave coupled equations in 1-temporal + 1-propagation dimensions [see, for example, Eq. (1) in Ref. [19]], i.e., in plane-wave approximation. Both the real and imaginary contributions of the cubic nonlinearity are included, according to the BBO-crystal coefficients given in Ref. [17]. Calculations are performed by taking as input condition a chirp-free pulse with spectrum and autocorrelation as close as possible to those in the experiment (see below the traces in Figs. 3a and 4a). The equations were numerically solved using a split-step approach, where the linear part was integrated in the Fourier space and the nonlinear part was integrated with a fourth-order Runge-Kutta algorithm, similar to that in Ref. [2]. By numerically solving the coupled equation in 2 (spatial and temporal) + 1 dimensions (data not shown; see results in Ref. [16]) we have verified the correctness of the adopted plane-wave approximation, in our large-beam operating regime.

In Fig. 1 we report numerical examples of the pulse-duration evolution inside the crystal, for typical operating conditions as in our experiment. As expected, for (large) positive Δk no solitons are obtained (in the regime of large $\Delta k \equiv k_{2\omega} - 2k_\omega$ bright solitons exist only for $k''_\omega \Delta k > 0$, in the absence of strong seeding [5]); for $\Delta k < 0$, in contrast, the injected pulse experiences a significant compression, followed by a dispersion-free regime, in which the pulse duration exhibits periodical oscillations.

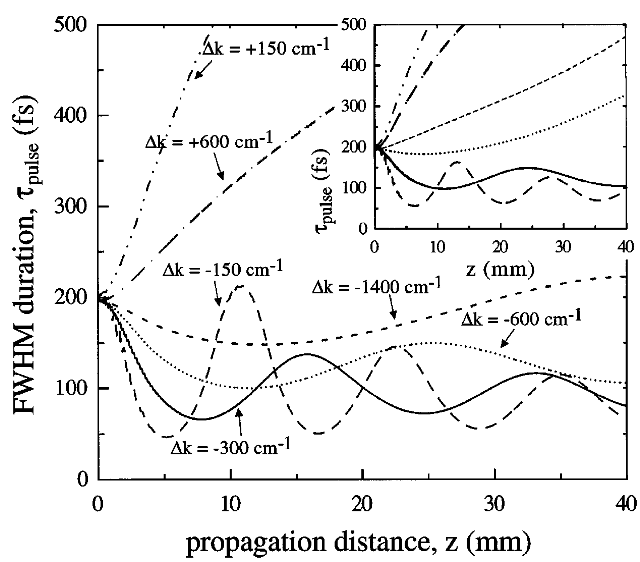

FIG. 1. Numerical results on the dynamics of tilted pulses in SHG out of phase matching, for different Δk. Crystal: type-I BBO; $I_{inp} = 13.4$ GW/cm^2; λ: 527 nm (fundamental); $\eta < 10\%$; tilt: 50°. Inset: results without $\chi^{(3)}$.

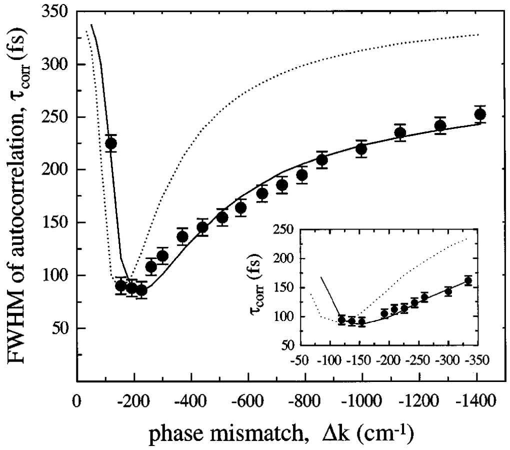

FIG. 2. Experimental (circles) and numerical (solid lines) results on the FWHM of SH autocorrelations of the output pulses. Crystal: 7-mm BBO; $I_{\text{inp}} = 13.4\ \text{GW/cm}^2$ (inset: $I_{\text{inp}} = 10.4\ \text{GW/cm}^2$); input-pulse duration: 200 fs ($\tau_{\text{corr}} = 284$ fs). Dotted lines: Numerical results without $\chi^{(3)}$.

The criterion adopted to verify the soliton-like regime of propagation relies upon the excellent and detailed agreement between experimental and numerical results, concerning the temporal and spectral features of the pulses exiting the crystal, for a wide range of input intensities (I_{inp}) and Δk parameters (this criterion is analogous to that used, in the space domain, in Refs. [2–4]). In Fig. 2 we plot the experimental and numerical FWHM of the output-pulse autocorrelations (τ_{corr}) vs Δk, for two different intensities (all with $\eta < 10\%$). In Table II (columns 5–8) we list the experimental (expt.) and numerical (num.) Δk leading to minimum duration ($\Delta k_{\min}$) with the corresponding τ_{corr}, for 5 different I_{inp} (and for input $\tau_{\text{corr}} = 284$ fs, as in Fig. 2). For comparison, we also report the numerical data obtained in the absence of (real) $\chi^{(3)}$ (columns 2 and 3) and $\chi^{(2)}$ (columns 4) contributions. In Figs. 3 and 4 we present the typical input (a) and output (b) pulse spectra and autocorrelations, at $\Delta k_{\min}$. The agreement between experimental and numerical results (Figs. 3b and 4b) is obtained without the aid of any free parameter (I_{inp} is deduced from the measured fluences *via* the pump-pulse shape which leads to the spectrum and autocorrelation in Figs. 3a and 4a; moreover, the beam in our experiment had a flat-top profile, which makes fluence measurements correct for the intensity estimation). The double-humped spectrum in Fig. 3(a) relates with the presence of pedestals in the (chirp-free) input-pulse temporal profiles, leading to the autocorrelation trace in Fig. 4(a). These pedestals arise in the nonlinear pulse compressor in which the input pulse is formed (see Fig. 1a in Ref. [18]). As confirmed by our calculations, solitons can be obtained also with Gaussian pulses of similar FWHM duration.

The numerical data in Table II ($\chi^{(2)} \neq 0$ and $\chi^{(3)} \neq 0$ section) show that, within ± 3 fs imprecision related to the

TABLE II. Output $\Delta k_{\min}$ and τ_{corr} at various I_{inp}.

	$\chi^{(3)} = 0$		$\chi^{(2)} = 0$	$\chi^{(2)} \neq 0$ and $\chi^{(3)} \neq 0$			
I_{inp} $[\frac{\text{GW}}{\text{cm}^2}]$	$\Delta k_{\min}$ [cm^{-1}]	τ_{corr} [fs]	τ_{corr} [fs]	$\Delta k_{\min}$ [cm^{-1}]		τ_{corr} [fs]	
	num.		num.	num.	expt.	num.	expt.
6.7	−57	88	329	−72.8	−72.8	80	104
7	−64	87	327	−85	−85	80	106
10.4	−120	88	305	−154	−154	86	90
13.4	−154	86	284	−226	−226	85	86
18.3	−205	85	249	−350	−350	83	88

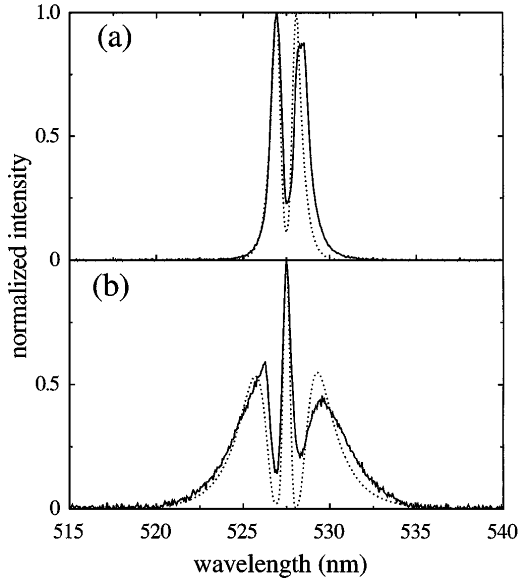

FIG. 3. Input (a) and output (b) pulse spectra. Experimental (solid lines) and numerical (dotted lines). Crystal: 7-mm BBO; $I_{\text{inp}} = 13.4\ \text{GW/cm}^2$; $\tau_{\text{pulse}} = 200$ fs; $\Delta k = -226\ \text{cm}^{-1}$.

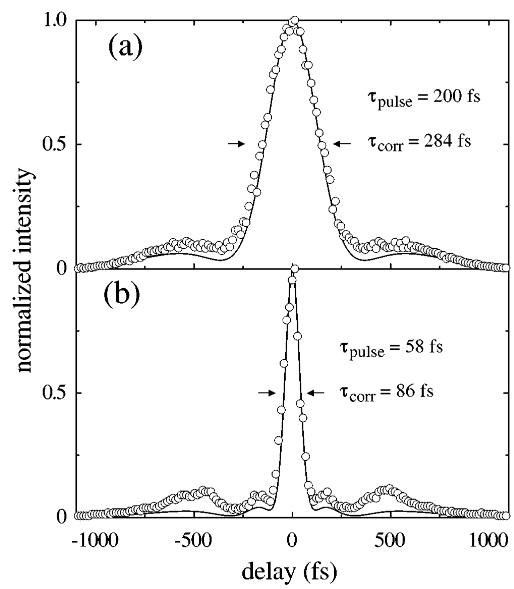

FIG. 4. Input (a) and output (b) pulse autocorrelations. Experimental (open circles) and numerical (solid lines). Input parameters as in Fig. 3.

grid in numerical calculations, the output pulses at $\Delta k_{\min}$ are expected to have the same duration for all I_{inp}, in the 6–18 GW/cm^2 range investigated. This prediction, which might turn out useful for applications, is well confirmed by the experimental data in the two scans in Fig. 2 (at $I_{\mathrm{inp}} = 10.4$ and 13.4 GW/cm^2) as well as by the point at $I_{\mathrm{inp}} = 18.3$ GW/cm^2 in Table II. Somewhat longer pulses than expected ($\simeq$20%) are obtained at $I_{\mathrm{inp}} = 6.7$ and 7 GW/cm^2. We relate this discrepancy occurring at small $\Delta k_{\min}$ with a residual GVM due to slightly incorrect tilt, whose impact on the output-pulse duration is expected to increase with the coherence length (numerical data; not shown). Note that, within the accuracy given by the (equal) numerical end experimental grids in Δk (see the examples in Fig. 2), the values of $\Delta k_{\min}$ coincide in the whole range of I_{inp}.

With regard to the role played by (real) $\chi^{(3)}$ in our experiment, it is worth noting that the negative GVD introduced by the tilt (see Table I) allows the $\chi^{(3)}$ to behave in support of the soliton formation. While 527 nm untilted pulses broaden in case of pure-$\chi^{(3)}$ interaction in BBO, a slight compression would take place at large I_{inp} in the case of tilt (see the output-pulse τ_{corr} in Table II, column 4). However, the effect cannot be considered the driving one in soliton generation: our numerical results show that the threshold for pure-$\chi^{(3)}$ solitons is $I_{\mathrm{inp}} = 22$ GW/cm^2 and that $I_{\mathrm{inp}} > 47$ GW/cm^2 is needed to obtain $\tau_{\mathrm{corr}} < 85$ fs. On the other hand, pure $\chi^{(2)}$ interaction would lead to almost the same minimum output durations as the $\chi^{(2)} + \chi^{(3)}$ case (compare columns 3 and 7, in Table II), the main effect of the $\chi^{(3)}$ contribution being that of increasing $\Delta k_{\min}$ (compare columns 2 and 5 in Table II; compare also the dotted and solid lines in Fig. 2), due to faster dynamics (see the inset in Fig. 1). The $\chi^{(3)}$ plays a more relevant role at larger Δk where, at our operating intensities, pure-$\chi^{(2)}$ solitons would be below threshold (compare the dynamics at -600 and $-1400\ \mathrm{cm}^{-1}$ in the inset in Fig. 1 with those in the main figure, at the same Δk). We mention that for $\Delta k > 0$ the interplay between the competing $\chi^{(2)}$ and $\chi^{(3)}$ nonlinearities can be investigated and interesting effects are expected [19] at higher intensities than those in our experiment.

In conclusion, we have shown that the tilt allows the generation of $\chi^{(2)}$ temporal solitons in phase-mismatched second-harmonic generation. Based on our numerical results, which provide a good quantitative agreement in the present regime, we expect that the process can be extended to quantum-noise parametric amplification, including the case of nondegenerate interaction. We believe that these results may find applications in both pulse-compression and light-by-light control devices.

The authors acknowledge A. Stabinis, G. Tamošauskas, and A. Visconti for precious discussions, help in experiment, and in calculations. P. Di Trapani is grateful to Wolfgang Rudolph for intriguing tutorial lectures on tilted pulses. The research has been partially supported by MURST Grant No. 9702268683-001 and CNR Grant No. 97.00070.CT02.

*Electronic address: DITRAPAN@FIS.UNICO.IT

[1] Yu. N. Karamzin and A. P. Sukhorukov, JETP Lett. **11**, 339 (1974).
[2] W. E. Torruellas, Z. Wang, D. J. Hagan, E. W. VanStryland, G. I. Stegeman, L. Torner, and C. R. Menyuk, Phys. Rev. Lett. **74**, 5036 (1995).
[3] R. Schiek, Y. Baek, and G. I. Stegeman, Phys. Rev. E **53**, 1138 (1996).
[4] P. Di Trapani, W. Chinaglia, and A. Andreoni, in *Proceedings of the European Quantum Electronics Conference (EQEC '96), Hamburg, Germany, 1996* (Report No. QWH1); P. Di Trapani, G. Valiulis, W. Chinaglia, and A. Andreoni, Phys. Rev. Lett. **80**, 265 (1998).
[5] G. Valiulis and K. Staliunas, Lith. J. Phys. **21**, 38 (1991); M. J. Werner and P. D. Drummond, Opt. Lett. **19**, 61 (1994); C. R. Menyuk, R. Schiek, and L. Torner, J. Opt. Soc. Am. B **11**, 2434 (1994); L. Torner, C. R. Menyuk, and G. I. Stegeman, Opt. Lett. **19**, 1615 (1994); A. V. Buryak and Y. S. Kivshar, Phys. Lett. A **197**, 407 (1995); L. Torner and E. M. Wright, J. Opt. Soc. Am. B **13**, 864 (1996); H. He, J. Werner, and P. D. Drummond, Phys. Rev. E **54**, 896 (1996).
[6] V. E. Zakharov and S. V. Manakov, Sov. Phys. JETP **42**, 842 (1976); E. Ibragimov and A. Struthers, J. Opt. Soc. Am. B **14**, 1472 (1997).
[7] S. A. Akhmanov *et al.*, IEEE J. Quantum Electron. **4**, 598 (1968).
[8] A. Staliunas, Lith. J. Phys. **28**, 637 (1988).
[9] O. E. Martinez, Opt. Commun. **59**, 229 (1986).
[10] R. Danielius, A. Piskarskas, P. Di Trapani, A. Andreoni, C. Solcia, and P. Foggi, Opt. Lett. **21**, 973 (1996).
[11] O. E. Martinez, IEEE J. Quantum Electron. **25**, 2464 (1989).
[12] G. Szabo and Zs. Bor, Appl. Phys. B **50**, 51 (1990).
[13] A. Dubietis, G. Valiulis, G. Tamošauskas, R. Danielius, and A. Piskarskas, Opt. Lett. **22**, 1071 (1997).
[14] A. Dubietis, G. Valiulis, G. Tamošauskas, R. Danielius, and A. Piskarskas, Opt. Commun. **144**, 55 (1997).
[15] S. Szatmari, P. Simon, and M. Feuerhake, Opt. Lett. **21**, 1156 (1996).
[16] G. Valiulis, A. Dubietis, R. Danielius, D. Caironi, A. Visconti, and P. Di Trampini (to be published).
[17] R. DeSalvo, A. A. Said, D. J. Hagan, E. W. Van Stryland, and M. Sheik-Bahae, IEEE J. Quantum Electron. **32**, 1324 (1996).
[18] R. Danielius, A. Dubietis, G. Valiulis, and A. Piskarskas, Opt. Lett. **20**, 2225 (1995).
[19] A. V. Buryak, Y. S. Kivshar, and S. Trillo, Opt. Lett. **20**, 1961 (1995).